Radio frequency field-induced persistent long-range ordered structures in two-species ion Coulomb crystals

2007 J. Phys. B: At. Mol. Opt. Phys. 40 F223

(http://iopscience.iop.org/0953-4075/40/15/F01)

IOP PUBLISHING | JOURNAL OF PHYSICS B: ATOMIC, MOLECULAR AND OPTICAL PHYSICS

J. Phys. B: At. Mol. Opt. Phys. **40** (2007) F223–F229 doi:10.1088/0953-4075/40/15/F01

FAST TRACK COMMUNICATION

Radio frequency field-induced persistent long-range ordered structures in two-species ion Coulomb crystals

A Mortensen, E Nielsen, T Matthey and M Drewsen

QUANTOP, Danish National Research Foundation Center for Quantum Optics, Department of Physics and Astronomy, University of Aarhus, DK-8000 Aarhus C, Denmark

E-mail: drewsen@phys.au.dk

Received 15 June 2007, in final form 4 July 2007
Published 25 July 2007
Online at stacks.iop.org/JPhysB/40/F223

Abstract

We report on the observations of strikingly persistent (lifetimes of ∼10 s) three-dimensional long-range ordered structures in the central $^{40}Ca^+$ ion component of $^{40}Ca^+$–$^{44}Ca^+$ two-species ion Coulomb crystals in a linear Paul trap. Molecular dynamics simulations strongly indicate that the observed structures are a hitherto unpredicted consequence of an effective anisotropy in the inter-particle interaction induced by the radio frequency quadrupole-trapping field. The results have implications for such diverse research fields as cold molecular ion studies and quantum information processing.

(Some figures in this article are in colour only in the electronic version)

When the nearest-neighbour Coulomb interaction energy in an ensemble of charged particles with the same sign of charge exceeds the thermal energy per particle by a factor of ∼200 [1–3], they form a solid state often referred to as a Wigner crystal or a Coulomb crystal. In particular laser-cooled trapped ions have proven to be excellent for studies of such crystals in the case of ions under various confinement conditions [4–14], and today ion Coulomb crystals find applications in a large variety of research fields spanning from frequency metrology [15, 16] over quantum information processing [17, 18] to cold molecular ion physical chemistry [19–23].

Ion Coulomb crystals have been investigated extensively both in Penning [4, 8, 9] and radio frequency (rf) traps (also named Paul traps) [5–7, 10–14]. For Penning traps, the trapping potential is equivalent to a cylindrically symmetric harmonic static potential in a rotating frame [24], and details of observed crystal structures have generally been found to be in very good agreement with molecular dynamics (MD) simulation results based on static potentials [11]. For rf quadrupole traps, in contrast, the trapping potential can only be *approximated* by a harmonic static potential, also named the pseudo-potential, under certain conditions and

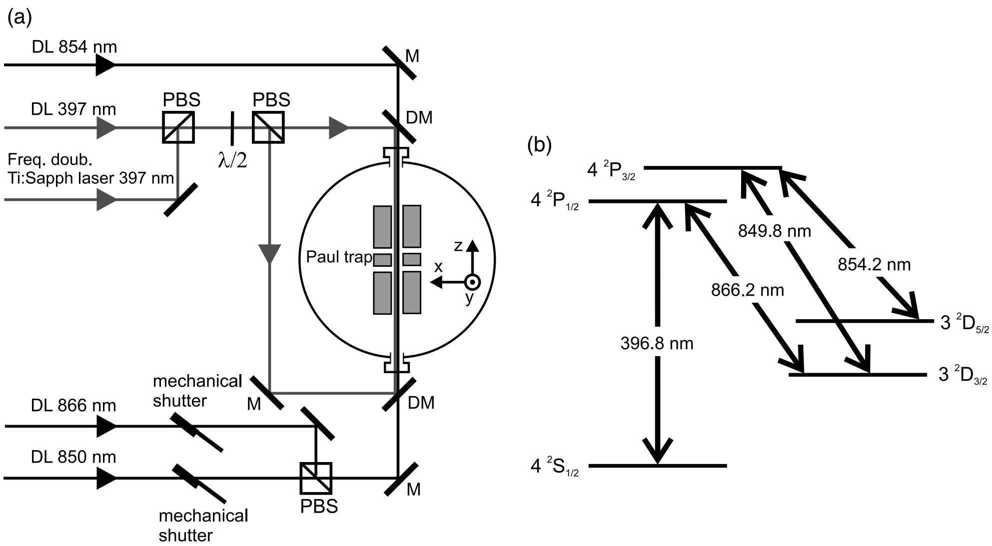

Figure 1. (a) Schematics of the laser and linear Paul trap setup. (D)M denotes a (dichroic) mirror, PBS denotes polarization beam splitters and DL denotes diode laser. (b) Optical transitions used for Doppler laser cooling of the Ca^+ ions.

when *averaged* over a rf period [5, 7]. While the pseudo-potential description has proven very efficient in describing large-scale characteristics, such as ion density, crystal shapes and shell structures, which have previously been observed [5–7, 11, 12], it is well known that the quadrupole nature of the trapping fields leads to an effective anisotropy in the inter-ion interactions, which can most simply be viewed in two-ion systems [25]. Since smaller ion Coulomb crystals in rf traps have already found applications in frequency metrology [15, 16], quantum computing [17, 18] and cold molecular ion research [19–23], and larger crystals in the near future can be expected to be exploited in cavity QED [26], quantum memory [27] as well as atomic/molecular ion cavity cooling [28] experiments, a better understanding of the effect of rf-induced anisotropic inter-ion interaction is certainly needed.

In this communication, we present observations of persistent long-range ordered structures in the $^{40}Ca^+$ component of a two-species crystal consisting of $^{40}Ca^+$ and $^{44}Ca^+$ ions, which we assign to the effective anisotropic inter-particle interaction induced by the applied rf quadrupole field of the linear trap. While the observed structures deviate from those expected from a pseudo-potential description [12, 29], they are in close agreement with results from molecular dynamics (MD) simulations including the quadrupole nature of the trapping fields.

The Ca^+ ions are confined in a linear Paul trap which is situated in a vacuum chamber at a pressure of 10^{-10} Torr, and are laser cooled as depicted in figure 1(a). The Paul trap used in these experiments has been described in detail elsewhere [20]. In short, the linear Paul trap consists of four electrode rods placed in a quadrupole configuration. The electrode diameter is 8.0 mm and the minimum distance to the central trap axis is $r_0 = 3.5$ mm. Time-varying voltages $\frac{1}{2}U_{\mathrm{rf}}\cos(\Omega_{\mathrm{rf}}t)$ and $-\frac{1}{2}U_{\mathrm{rf}}\cos(\Omega_{\mathrm{rf}}t)$ are applied to the two sets of diagonally opposite electrode rods, respectively, to obtain confinement in the radial plane (xy-plane in figure 1(a)). Axial confinement along the z-axis is accomplished by sectioning each of the electrode rods into three pieces and applying a static voltage U_{end} to the end electrodes. The length of the centre electrode is 5.4 mm, while the outer pieces are 20 mm. In the present experiments $\Omega_{\rm rf} = 2\pi \times 3.88$ MHz, $U_{\rm rf} \sim 540$ V and $U_{\rm end} \sim 10$–50 V were used. The resulting approximative pseudo-potential for an ion species of type i with mass M_i and charge Q_i is given by $\Phi_{\rm ps}(r, z) = \frac{1}{2}M_i\left(\omega_{\rm r}^2 r^2 + \omega_z^2 z^2\right)$, where $\omega_{\rm r}$ and $\omega_{\rm z}$ are the radial and axial trap frequencies, respectively. The axial trap frequency is given by $\omega_z^2 = 2\kappa Q_i U_{\rm end}/M_i$, where $\kappa = 3.97 \times 10^4$ m^{-2} is a constant related to trap geometry, and the time-averaged radial trap frequency is given by $\omega_r^2 = \omega_{\rm rf}^2 - \frac{1}{2}\omega_z^2$, where $\omega_{\rm rf}^2 = Q_i^2 U_{\rm rf}^2 / 2M_i r_0^4 \Omega_{\rm rf}^2$ is the contribution from the time-varying quadrupole fields. The dependence on the charge and mass of the ion species makes the lighter isotope (^{40}Ca$^+$) more tightly bound towards the trap axis than the heavier (^{44}Ca$^+$) and leads consequently to a total radial separation of the two ion species when sufficiently cooled [12]. The zero-temperature ion density in the pseudo-potential is given by $n_{\rm theo} = \epsilon_0 U_{\rm rf}^2 / M_i r_0^4 \Omega_{\rm rf}^2$, where ϵ_0 is the vacuum permittivity [12]. Due to the spatial separation of the ions in two-species ion Coulomb crystals, this expression is also applicable to the individual components of such crystals.

The ^{40}Ca$^+$ and ^{44}Ca$^+$ ions used in the experiments are produced isotope selectively by resonant two-photon photo-ionization of atoms in an effusive beam of naturally abundant calcium [30, 31]. In figure 1(b), the transitions in Ca$^+$ used for Doppler laser cooling of the trapped ions are shown. The main cooling transition is the dipole-allowed $4S_{1/2} \rightarrow 4P_{1/2}$ transition at 397 nm. To avoid optical pumping into the metastable $3D_{3/2}$ state, repumping is done either by using a single repump laser at 866 nm via the $4P_{1/2}$ state (^{44}Ca$^+$) or by using two repump lasers at 850 nm and 854 nm via the $4P_{3/2}$ state (^{40}Ca$^+$). The different repumping schemes are simply introduced for technical reasons. Due to the isotope shifts of the order of GHz of the cooling transitions [6, 32], each isotope ion requires its own laser-cooling frequencies. As indicated in figure 1(a), we use a 397 nm frequency doubled Ti:Sapphire laser and a 866 nm diode laser for the cooling of ^{44}Ca$^+$ ions, while for the ^{40}Ca$^+$ ions 397 nm, 850 nm and 854 nm diode lasers are applied. For both isotopes the final temperature is of the order of $\sim$10 mK, which is low enough for achieving Coulomb crystallization ($\Gamma \sim 250$ [3]). Projection images of the trapped ions are obtained by detecting the flourescence light by an image-intensified CCD camera. Using the cylindrical symmetry of the pseudo-potential and the equation for $n_{\rm theo}$, from such images, the number of the individual ion species in the Coulomb crystals can be determined [33].

Projection images of two-species Coulomb crystals consisting of ^{40}Ca$^+$ and ^{44}Ca$^+$ ions are presented in figure 2 for various settings of the static voltage $U_{\rm end}$ on the end electrodes. Since the ions are only fluorescing when they are directly laser cooled, the two isotopes can be imaged separately by alternating blocking (about 1 Hz rep. rate) the 850 nm (^{40}Ca$^+$ laser cooling off) and the 866 nm laser (^{44}Ca$^+$ laser cooling off) using mechanical shutters. The presented combined images are subsequently created with a red colour coding for ^{40}Ca$^+$ and blue for ^{44}Ca$^+$. Due to sympathetic cooling [4, 10], the crystal retains its shape and structure during the alternating laser-cooling sequence. As expected [12], the lightest isotope ^{40}Ca$^+$ is located as a cylindrical core closest to the trap axis, surrounded by the heavier ^{44}Ca$^+$. It is immediately clear from the images in figure 2 that the projection of the actual three-dimensional structure of the ^{40}Ca$^+$ ions is a two-dimensional rectangular pattern aligned with the trap axis. Since the depth of focus of the imaging system ($\sim$50 μm) is several times the inter-ion distance, we conclude the rectangular pattern in the projection images must originate from a three-dimensional long-range ordering [14]. In contrast to our previous observations of long-range order in spherical one-component ion crystals [14], where the orientation of the observed metastable ($\sim$100 ms) structures seemed to be arbitrary, the rectangular patterns presented here are very persistent ($\sim$10 s) and always oriented the same way. Accordingly, the presence of the surrounding ^{44}Ca$^+$ ions apparently has significant influence on the formation and appearance of the observed long-range ordered structure in the ^{40}Ca$^+$ part of the crystal.

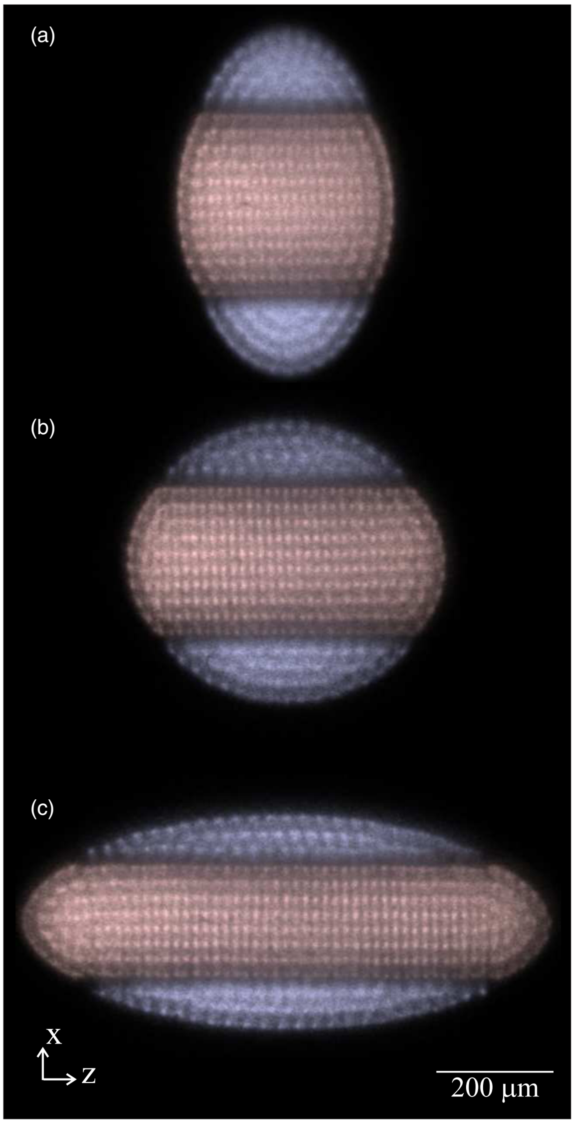

Figure 2. Projection images of two-species ion Coulomb crystals containing $\sim$1500 $^{40}Ca^{+}$ ions (red) and $\sim$2000 $^{44}Ca^{+}$ ions (blue) at different settings of the end-cap potential, U_{end}. The camera exposure time is $\sim$100 ms and the trap potentials are $U_{\mathrm{rf}} = 540$ V and (a) $U_{\mathrm{end}} = 46.1$ V, (b) $U_{\mathrm{end}} = 30.2$ V and (c) $U_{\mathrm{end}} = 13.8$ V, respectively.

The lifetime of the observed persistent structures might possibly be limited by infrequent collisions with background gas atoms or molecules. The image sequence in figure 2 illustrates additionally that despite changes in the outer shape of the $^{40}Ca^{+}$ core, the observed rectangular pattern of the ions is preserved, indicating that the observed long-range ordered structure is rather stable to changes in the boundary conditions of the crystal as well as to the absolute amplitude of the rf-induced micromotion which scales linearly with the distance from the centre axis of the trap [14].

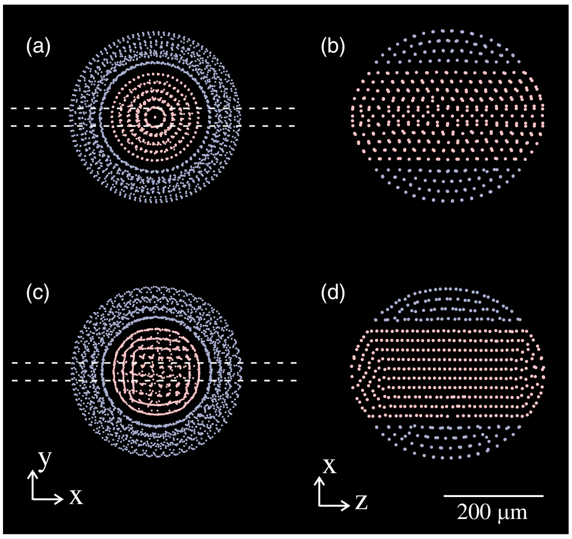

Figure 3. MD simulation data of a two-species ion Coulomb crystal containing 1500 $^{40}Ca^{+}$ ions (red) and 2000 $^{44}Ca^{+}$ ions (blue) using a pseudo-potential approximation ((a) and (b)) and using the full rf potential ((c) and (d)), respectively. While (a) and (c) show a projection of all the ion positions onto the xy-plane, (b) and (d) present the data points contained in a slice of thickness 24 μm through the crystal centre projected to the xz-plane. The slices are indicated by white dashed lines in (a) and (c). Trap potentials are $U_{\mathrm{rf}} = 540$ V and $U_{\mathrm{end}} = 33$ V.

In order to understand the observations, a series of molecular dynamics (MD) simulations of two-species crystals with the same number of the two calcium isotope ions as in the crystals shown in figure 2 have been performed. In figures 3(a) and (b), results from one simulation using a pseudo-potential corresponding to the trapping parameters of figure 2(b) are presented. As in the experiments, a clear radial separation of the two isotope ions is observed. Furthermore the radial projection (figure 3(a)) clearly reveals that the $^{40}Ca^{+}$ part of the crystal is organized in concentric cylindrical structures, resembling the structure of an infinitely long 1D cylindrically symmetric confined ion crystal [12, 29]. In figure 3(b), a projection corresponding to the focal region of the imaging system is shown. Neither this nor other sections, e.g., in the yz-plane, lead to projection images with rectangular patterns. However, when the full rf potential is used in the MD simulations, some long-range ordering in the central component of the crystal does appear, as is evident from the results presented in figures 3(c) and (d) for a specific phase of the rf field. From figure 3(d), it is seen that indeed a rectangular pattern in the projection image is expected when the rf-quadrupole field, which breaks the cylindrical symmetry, is included in the simulations. Even when averaging over all phases of the rf field, the rectangular pattern persists. However, some blurring of the position of the ions along the x-axis, as is seen in the projection images of figure 2, is then found. Analysis of a much simpler two-ion system in a linear rf trap has previously shown similar preferred orientation effects with respect to the rf quadrupole field axes [34].

A closer analysis of the simulation results presented in figures 3(c) and (d) shows that the $^{40}Ca^{+}$ ions in the core organize themselves in a long-range ordered structure in the form of a face-centred tetragonal (fct) lattice as illustrated in figure 4(a), with the side lengths related by $a = b = \sqrt{3}c$. The rectangular pattern in the projection presented in figure 3(d) is obtained when the fct structure is viewed along the b vector as illustrated in figure 4(b). This rectangular

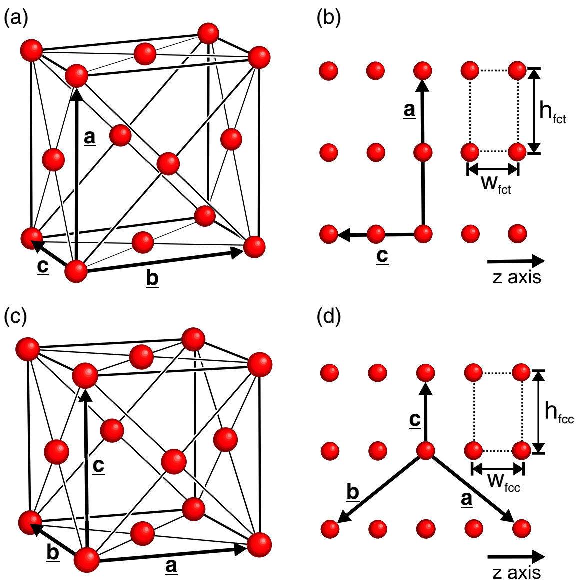

Figure 4. Fct lattice cell (a) with projection along the *b* vector (b). Fcc lattice cells (c) with projection along the [2 1 1]-direction (d).

pattern has a height to width ratio of $h_{\mathrm{fct}}/w_{\mathrm{fct}} = \sqrt{3} \simeq 1.73$, which is not exactly the same as the $h/w = 1.62 \pm 0.07$ observed in the experiments. In fact, the observed rectangular pattern is more in agreement with a face-centred cubic (fcc) structure viewed along the [2 1 1] direction (see figures 4(c) and (d)), which would lead to $h_{\mathrm{fcc}}/w_{\mathrm{fcc}} = \sqrt{8/3} \simeq 1.63$. The reason for the deviation between the simulated results and the actually observed structures is probably that the difference in the potential energies of the two structures in the rf potential is very small, as is well known to be the case for various long-range ordered structures in infinite systems without the presence of rf fields [2]. In recent single component experiments both body-centred cubic (bcc) and fcc-like structures were indeed observed [14], but in contrast to the two-species results above, no fixed orientation with respect to the trap axis was found. Another point supporting that the observed structure is a fcc structure is the ion density. Assuming that the observed projection images of $^{40}Ca^+$ ions in figure 2 are actually fcc structures observed along the [2 1 1] direction, the ion density must be $n_{\mathrm{fcc}} = (3.8 \pm 0.4) \times 10^8$ cm^{-3}. In comparison, the $^{40}Ca^+$ ion density calculated from the trap parameters is $n_{\mathrm{theo},40} = (4.3 \pm 0.3) \times 10^8$ cm^{-3}, in good agreement with the fcc assumption.

Very stable aligned crystal structures as those discussed above may have future applications within several fields. Cavity cooling of molecular ions [28] may, e.g., benefit from having vibrational transitional wavelengths in the vicinity of the axial ion spacing or an integer multiple of thereof, since the collective coupling of the molecular ensemble to the light field can then be controlled by shifting the position of the whole crystal. For extremely regular axial ion spacing, such structural effects may even be exploited in cavity QED studies [26] using atomic ions and visible light. Finally, from a quantum memory point of view, the evidently slow ion diffusion in the regular structures may enhance the time over which quantum information can be stored.

In conclusion, a very persistent three-dimensional long-range ordered structure with one specific orientation with respect to the symmetry axis of the rf field have been observed in the central component of a two-species ion Coulomb crystals in a linear Paul trap. MD simulations strongly indicate that these characteristics are a consequence of the effective anisotropy in the inter-particle interaction induced by the applied rf quadrupole field. Since similar stable structures are not observed for single-species Coulomb crystals, the coinciding symmetry axis of the rf-field and the central ion component of the Coulomb crystal must play a crucial role.

Acknowledgments

We acknowledge financial support from the Carlsberg Foundation.

References

[1] Pollock E L and Hansen J P 1973 *Phys. Rev.* A **8** 3110
[2] Dubin D H E 1989 *Phys. Rev.* A **40** 1140
[3] Schiffer J P 2002 *Phys. Rev. Lett.* **88** 205003
[4] Larson D J, Bergquist J C, Bollinger J J, Itano W M and Wineland D J 1986 *Phys. Rev. Lett.* **57** 70
[5] Birkl G, Kassner S and Walther H 1992 *Nature* **357** 310
[6] Alt W, Block M, Schmidt V, Nakamura T, Seibert P, Chu X and Werth G 1997 *J. Phys. B: At. Mol. Opt. Phys.* **30** L677
[7] Drewsen M, Brodersen C, Hornekær L, Hangst J S and Schiffer J P 1998 *Phys. Rev. Lett.* **81** 2878
[8] Mitchell T B, Bollinger J J, Dubin D H E, Huang X P, Itano W M and Baughman R H 1998 *Science* **282** 1290
[9] Itano W M, Bollinger J J, Tan J N, Jelenković B, Huang X P and Wineland D J 1998 *Science* **279** 686
[10] Bowe P, Hornekær L, Brodersen C, Drewsen M, Hangst J S and Schiffer J P 1999 *Phys. Rev. Lett.* **82** 2071
[11] Schätz T, Schramm U and Habs D 2001 *Nature* **412** 717
[12] Hornekær L, Kjærgaard N, Thommesen A M and Drewsen M 2001 *Phys. Rev. Lett.* **86** 1994
[13] Blythe P, Roth B, Frohlich U, Wenz H and Schiller S 2005 *Phys. Rev. Lett.* **95** 183002
[14] Mortensen A, Nielsen E, Matthey T and Drewsen M 2006 *Phys. Rev. Lett.* **96** 103001
[15] Schmidt P O, Rosenband T, Langer C, Itano W M, Bergquist J C and Wineland D J 2005 *Science* **309** 749
[16] Oskay W H *et al* 2006 *Phys. Rev. Lett.* **97** 020801
[17] Riebe M *et al* 2004 *Nature* **429** 734
[18] Barrett M D *et al* 2004 *Nature* **429** 737
[19] Mølhave K and Drewsen M 2000 *Phys. Rev.* A **62** 011401
[20] Drewsen M, Jensen I, Lindballe J, Nissen N, Martinussen R, Mortensen A, Staanum P and Voigt D 2003 *Int. J. Mass Spectrom.* **229** 83
[21] Bertelsen A, Jørgensen S and Drewsen M 2006 *J. Phys. B: At. Mol. Opt. Phys.* **39** L83
[22] Roth B, Koelemeij J C J, Daerr H and Schiller S 2006 *Phys. Rev.* A **74** 040501
[23] Ostendorf A, Zhang C B, Wilson M A, Offenberg D, Roth B and Schiller S 2006 *Phys. Rev. Lett.* **97** 243005
[24] Bollinger J J, Heinzen D J, Moore F L, Itano W M, Wineland D J and Dubin D H E 1993 *Phys. Rev.* A **48** 525
[25] Moore M G and Blümel R 1994 *Phys. Rev.* A **50** R4453
[26] Herskind P, Mortensen A, Sørensen J L and Drewsen M 2006 *Non-Neutral Plasma Physics VI* vol 862 ed M Drewsen *et al* (New York: AIP) p 292
[27] Mortensen A, Jensen F, Voigt D and Drewsen M 2003 *Coherence and Quantum Optics VIII* ed N Bigelow *et al* (Dordrecht/New York: Kluwer/Plenum) p 343
[28] Vuletić V and Chu S 2000 *Phys. Rev. Lett.* **84** 3787
[29] Hasse R W and Schiffer J P 1990 *Ann. Phys.* **203** 419
[30] Kjærgaard N, Hornekær L, Thommesen A, Videsen Z and Drewsen M 2000 *Appl. Phys.* B **71** 207
[31] Mortensen A, Lindballe J J T, Jensen I S, Staanum P, Voigt D and Drewsen M 2004 *Phys. Rev.* A **69** 042502
[32] Mårtensson-Pendrill A M, Ynnerman A, Warston H, Vermeeren L, Silverans R E, Klein A, Neugart R, Schulz C and Lievens P and The ISOLDE Collaboration 1992 *Phys. Rev.* A **45** 4675
[33] Madsen D N, Balslev S, Drewsen M, Kjærgaard N, Videsen Z and Thomsen J W 2000 *J. Phys. B: At. Mol. Opt. Phys.* **33** 4981
[34] Drewsen M and Brøner A 2000 *Phys. Rev.* A **62** 045401